Biochemical and Biophysical Research Communications 388 (2009) 21–27

Contents lists available at ScienceDirect

Biochemical and Biophysical Research Communications

journal homepage: www.elsevier.com/locate/ybbrc

Dual roles of a conserved pair, Arg23 and Ser20, in recognition of multiple substrates in α-aminoadipate aminotransferase from *Thermus thermophilus*

Takuya Ouchi [a], Takeo Tomita [a], Tomoharu Miyagawa [a], Tomohisa Kuzuyama [a], Makoto Nishiyama [a,b,*]

[a] *Biotechnology Research Center, The University of Tokyo, 1-1-1 Yayoi, Bunkyo-ku, Tokyo 113-8657, Japan*
[b] *RIKEN SPring-8 Center, 1-1-1 Kouto, Sayo-cho, Sayo-gun, Hyogo 679-5148, Japan*

ARTICLE INFO

Article history:
Received 15 July 2009
Available online 24 July 2009

Keywords:
Aminotransferase
Crystal structure
Lysine biosynthesis
Substrate specificity

ABSTRACT

To clarify the mechanism for substrate recognition of α-aminoadipate aminotransferase (AAA-AT) from *Thermus thermophilus*, the crystal structure of AAA-AT complexed with *N*-(5′-phosphopyridoxyl)-L-glutamate (PPE) was determined at 1.67 Å resolution. The crystal structure revealed that PPE is recognized by amino acid residues the same as those seen in *N*-(5′-phosphopyridoxyl)-L-α-aminoadipate (PPA) recognition; however, to bind the γ-carboxyl group of Glu at a fixed position, the Cα atom of the Glu moiety moves 0.80 Å toward the γ-carboxyl group in the PPE complex. Markedly decreased activity for Asp can be explained by the shortness of the aspartyl side chain to be recognized by Arg23 and further dislocation of the Cα atom of bound Asp. Site-directed mutagenesis revealed that Arg23 has dual functions for reaction, (i) recognition of γ (δ)-carboxyl group of Glu (AAA) and (ii) rearrangement of α2 helix by changing the interacting partners to place the hydrophobic substrate at the suitable position.

Introduction

Lysine was believed to be synthesized through the diaminopimelate pathway in bacteria and plants [1] with the only exception in lower eukaryotes through α-aminoadipate (AAA) [2,3]. In previous studies we found that the extremely thermophilic bacterium, *Thermus thermophilus,* synthesizes lysine through AAA [4]. The *Thermus* pathway is unique in that the latter part of the pathway, from AAA to lysine, is similar to the arginine biosynthetic pathway [5], but differs from that in lower eukaryotes with saccharopine as an intermediate. Since our discovery, lysine biosynthesis through AAA has been suggested to be spread in prokaryotes, especially hyperthermophilic archaea [6,7].

α-Aminoadipate aminotransferase (AAA-AT, EC 2.6.1.39) catalyzes pyridoxal 5′-phosphate (PLP)-dependent transamination using 2-oxoadipate as an amino acceptor to yield AAA in lysine biosynthesis of *T. thermophilus* (Fig. 1A). AAA-AT also utilizes various amino acids; for example, AAA, Glu, Leu, Phe, and kynurenine (Fig. 1B); therefore, AAA-AT may contribute not only to lysine biosynthesis, but also to other metabolisms [8]. In order to elucidate the mechanism of multiple-substrate recognition, we have determined the crystal structures of AAA-AT in four forms: PLP complex, PLP/Leu complex, *N*-(5′-phosphopyridoxyl)-L-leucine (PPL) complex, and *N*-(5′-phosphopyridoxyl)-L-α-aminoadipate (PPA) complex [9]. Structural studies for AAA-AT revealed that multiple-substrate recognition is ascribed to the high flexibility of α2 helix to take multiple conformations depending on substrates; for example, α2 helix is displaced 5.3 Å and 5.9 Å in PPA and PPL complexes, respectively, compared to the corresponding helix of the PLP complex. In the PPA complex, Arg23 on the helix extends its side chain to the active site to make salt bridges with δ-carboxylate of AAA, while in the PPL complex, Arg23 flipped toward the outside of the active site, to orient the hydrophobic face of α2 helix to the active site. AAA-AT uses Glu as the amino donor in lysine biosynthesis; however, we have not yet determined how AAA-AT recognizes Glu. Here, we report the crystal structure of AAA-AT in complex with *N*-(5′-phosphopyridoxyl)-L-glutamate (PPE) at 1.67 Å resolution. To verify the multiple-substrate recognition mechanism, we introduced point mutations into α2 helix and analyzed their kinetic parameters.

Materials and methods

Crystallization of PPE complex. For crystallization, recombinant AAA-AT was expressed in *E. coli* BL21 (DE3) CodonPlus® RIL and purified by the method described previously [8]. Ammonium sul-

Abbreviations: AAA, α-aminoadipic acid; PPA, *N*-(5′-phosphopyridoxyl)-L-α-aminoadipic acid; PPE, *N*-(5′-phosphopyridoxyl)-L-glutamic acid; PPL, *N*-(5′-phosphopyridoxyl)-L-leucine; AAA-AT, α-aminoadipate aminotransferase; TCA, tricarboxylic acid; 2-OG, 2-oxoglutaric acid; PEG, polyethylene glycol; HEPES, 4-(2-hydroxyethyl)-1-piperazineethanesulfonic acid

* Corresponding author. Address: Biotechnology Research Center, The University of Tokyo, 1-1-1 Yayoi, Bunkyo-ku, Tokyo 113-8657, Japan. Fax: +81 3 5841 8030.
E-mail address: umanis@mail.ecc.u-tokyo.ac.jp (M. Nishiyama).

0006-291X/$ - see front matter © 2009 Elsevier Inc. All rights reserved.
doi:10.1016/j.bbrc.2009.07.096

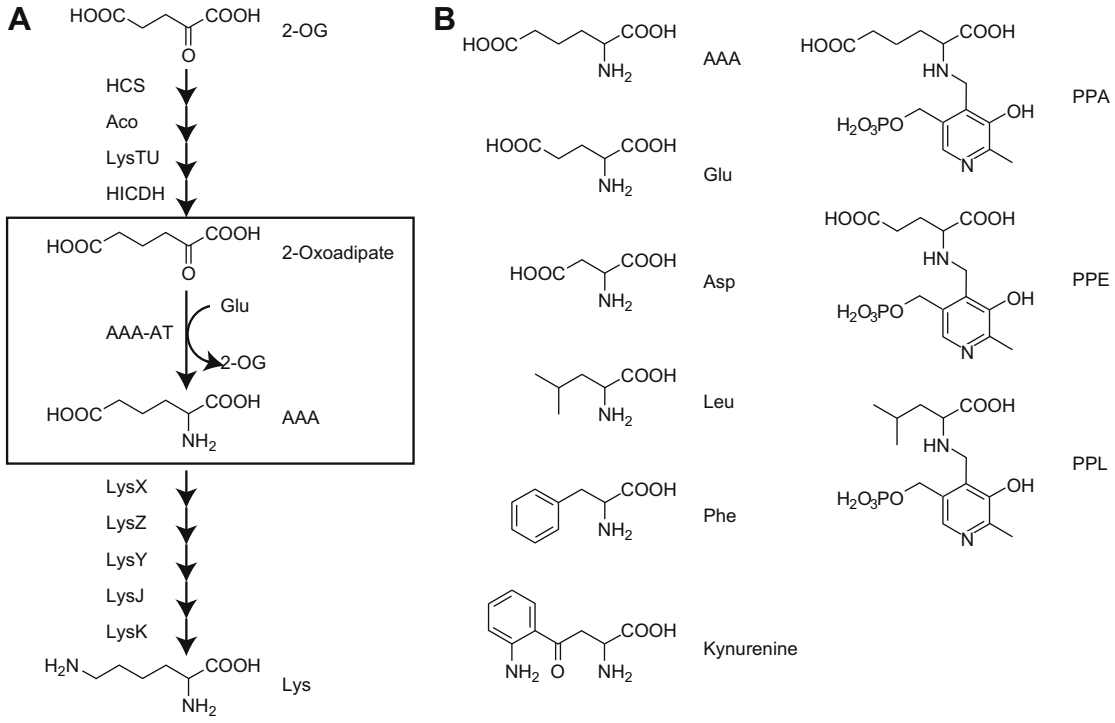

Fig. 1. Lysine biosynthetic pathway of *Thermus thermophilus* (A) and chemical structures of substrates or substrate analogs for AAA-AT (B). The reaction catalyzed by AAA-AT is boxed.

fate was added to the purified enzyme solution at a final 65% saturation. After 1 h incubation followed by centrifugation at 40,000*g*, the precipitated proteins were suspended in 10 ml of 1.0 M potassium phosphate buffer, pH 7.0, containing 10 mM Glu and kept at 25 °C for 12 h to convert PLP attached to AAA into PMP [10]. The protein solution was dialyzed against 1 l of 20 mM Tris–HCl, pH 8.0, three times to obtain apo-enzyme. The dialyzed protein solution was applied to a Hi-load 16/60 Superdex 200 prep-grade column (GE Healthcare) equilibrated with 20 mM Tris–HCl, pH 8.0. The external-aldimine-like analog, PPE, was synthesized by the method of Islam et al. [11]. The purified protein was concentrated to 10 mg/ml and treated with 20-fold excess in a molar ratio of PPE at 45 °C for 1 h to form PPE complex. The enzyme was crystallized by the vapor diffusion method at 20 °C by mixing 1 μl of the protein solution with an equal volume of a reservoir solution. High-quality crystals were obtained in a few days using 16% PEG3350 (w/v), 100 mM HEPES, pH 7.0, and 200 mM calcium acetate as the reservoir.

Data collection and processing. Before data collection, the crystals were transferred to a series of reservoir solutions finally supplemented with a cryoprotectant, 20% PEG 400 (w/v), by increasing the concentration of the cryoprotectant by 5% in each step, with equilibration for about 1 min between steps. Crystals were flash-frozen in a cold N_2 stream from a liquid-nitrogen cryostat (Rigaku, Tokyo, Japan). Diffraction data sets were collected with an ADSC Quantum CCD detector on the BL6A station at the Photon Factory in High Energy Accelerator Research Organization (KEK). All data

Table 1
Oligonucleotide primers used for site-directed mutagenesis.

Primer	Sequence
S20E-Fw	5′-GGAAGGATCCAGGCCGAGACCATCCGGGAG-3′
S20E-Rv	5′-CTCCCGGATGGTCTCGGCCTGGATCCTTCC-3′
R23Q-Fw	5′-CAGGCCTCCACCATCCAGGAGCTTCTCAAG-3′
R23Q-Rv	5′-CTTGAGAAGCTCCTGGATGGTGGAGGCCTG-3′
R23A-Fw	5′-CAGGCCTCCACCATCGCGGAGCTTCTCAAG-3′
R23A-Rv	5′-CTTGAGAAGCTCCGCGATGGTGGAGGCCTG-3′

Table 2
Data collection and refinement statistics.

Data collection	
Beamline	PF BL-6A
Space group	$P2_12_12_1$
Cell dimensions	
a (Å)	55.8
b (Å)	93.3
c (Å)	150.8
Resolution (Å)[a]	1.67 (1.67–1.73)
Total reflections	572,884
Unique reflections	91,922
Completeness (%)[a]	99.2 (99.8)
Average $I/\sigma(I)$[a]	14.2 (2.2)
R_{merge} (%)[a,b]	9.7 (58.8)
Refinement	
Resolution (Å)	30.47–1.67
R-factor/R_{free} (%)	19.3/24.6
No. of protein atoms	6,337
No. of ligands	2
No. of water molecules	956
Average B-factor (Å^2)	
Protein	22.8
Water	21.5
PPE	22.7
R.m.s.d. from ideal values	
Bond length (Å)	0.014
Bond angles (deg.)	1.5
Ramachandran plot (%)	
Favored	93.1
Additional allowed	6.1
Generally allowed	0.5
Disallowed	0.3

[a] Values in parentheses are for the highest resolution shell.
[b] $R_{merge} = \Sigma|I_i - \langle I\rangle|/\Sigma\langle I\rangle$.

sets were collected at 95 K from a single crystal mounted on a cryoloop. Diffraction images were indexed, integrated, and scaled with HKL2000 [12]. The structure of the PPE complex was determined by molecular replacement with the program MOLREP [13] in the CCP4 program suite [14] using the AAA-AT/PPA complex as the search model (PDB ID 3CBF). Model correction on the electron density map was performed with Coot [15]. Refinement was performed with Refmac5.2 [16]. The final model contains two monomers in an asymmetric unit. Data collection and refinement statistics and the results of Ramachandran plots produced by the program PROCHECK [17] are summarized in Table 1. Although Leu268 falls in the disallowed region, excellent map fitting ensures unambiguous model building. Figures were prepared using Pymol [http://pymol.sourceforge.net/]. The atomic coordinates of the PPE complexes have been deposited in the RCSB PDB with accession number 2ZYJ.

Preparation of AAA-AT and mutants. S20E, R23Q and R23A mutant genes were prepared using His-tagged wild-type AAA-AT as a template by a QuikChange kit (Stratagene-Japan) using the oligonucleotide primers listed in Table 2. Each mutant with a correct sequence was introduced into the expression vector, pET-26b(+). The mutants and wild-type AAA-AT were expressed, purified, and concentrated as described in a previous report [9]. The purity of proteins was verified by sodium dodecylsulfate–polyacrylamide gel electrophoresis (12%). The concentrations of proteins were determined by the method of Bradford using a protein assay kit (Nippon Bio-Rad).

Enzyme assay. The enzyme reaction was initiated by adding an appropriate amount of the enzyme to 1 ml reaction buffer, which was preincubated at 45 °C for 5 min. When 2-oxoglutarate (2-OG) was used as an amino acceptor and AAA or Leu was used as an amino donor, the reaction mixture contained 50 mM HEPES-NaOH buffer, pH 8.0, 50 mM KCl, 0.15 mM pyridoxal 5′-phosphate, 3 mM NAD^+, 11.9 U glutamate dehydrogenase, 0.05–5 mM 2-OG, and 0.1–10 mM AAA or Leu. When 2-oxoisocaproate was used as an amino acceptor and Glu was used as an amino donor, reactions were performed in 50 mM HEPES–NaOH buffer, pH 8.0, containing 50 mM NH_4Cl, 0.15 mM pyridoxal 5′-phosphate, 0.15 mM NADH, 11.9 U glutamate dehydrogenase, 0.1–10 mM 2-oxoisocaproate, and 0.05–5 mM Glu. The reaction was performed at 45 °C by monitoring absorbance at 340 nm of NADH. Kinetic parameters were calculated using an initial velocity program, HYPER [18]. One unit of enzyme activity was defined as the amount of enzyme that reduced 1 μmol NADH per min at 45 °C in the reaction.

Results and discussion

Structure of the PPE complex

The structure of AAA-AT with PPE was determined at 1.67 Å resolution. A model from Met 1 to Val 397 was built. The electron density map for PPE is shown in Fig. 2A. The backbone structure of the PPE complex is almost identical to that of the PPA complex with an r.m.s.d. value of 0.25 Å for 794 Cα atoms (Fig. 2B). The α-carboxyl

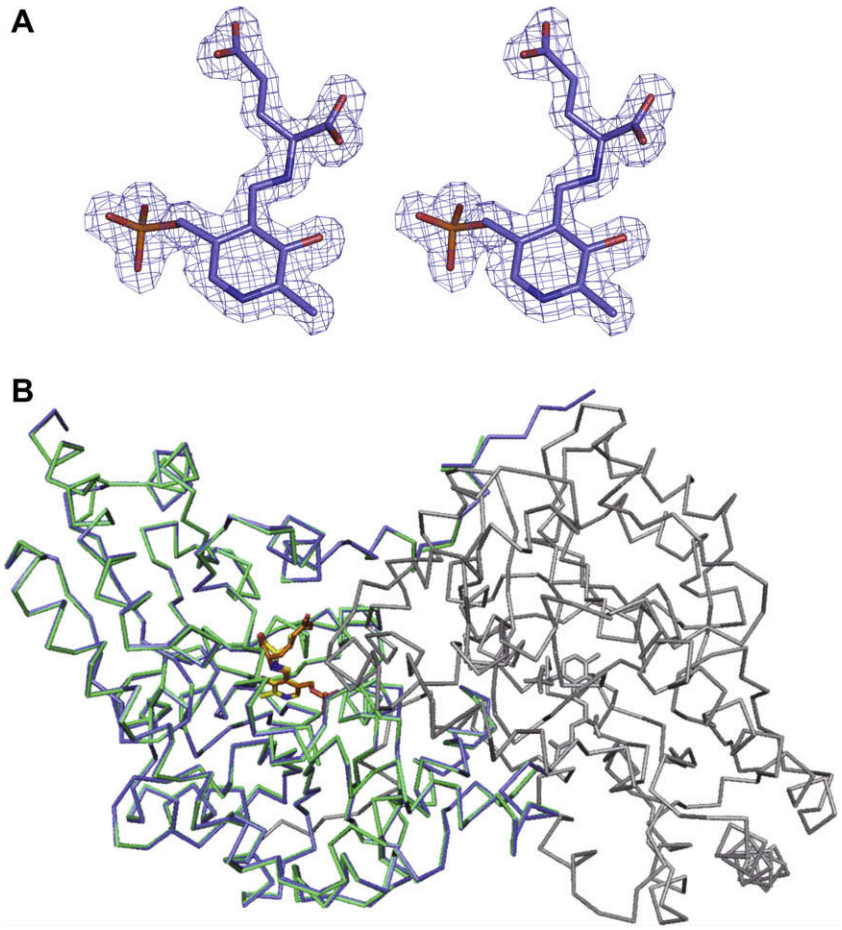

Fig. 2. Crystal structure of AAA-AT/PPE complex. (A) A stereo diagram of PPE in A chain shown as a stick model. The F_o–F_c omit map of PPE contoured at 3.0σ is shown in purple. (B) The overall structure of the PPE complex superposed on the PPA complex. A chain of the PPE complex, A chain of the PPA complex, and the B chain of the PPE complex are in purple, green and gray, respectively. The bound ligands, PPE and PPA, are shown as stick models in yellow and orange, respectively.

group of the Glu moiety of PPE forms salt bridges with Arg368 and hydrogen bonds with Gly40 and Asn174, and the γ-carboxyl group of the Glu moiety of PPE forms salt bridges with Arg23 (Fig. 3A). Four water molecules are present in the active site and stabilize the recognition of PPE by nearby residues. Although Glu is one methylene unit shorter than AAA, the recognition of PPE is quite similar to that of PPA (Fig. 3A). In the PPE complex, the guanidinium group of Arg23 is displaced only 0.3 Å, compared with that in the PPA complex, and forms hydrogen bonds with Ser71*, Thr73*, and Leu268* (asterisks indicate residues from another subunit), as seen in the PPA complex.

The γ-carboxyl group of the Glu moiety of PPE and the δ-carboxyl group of the AAA moiety of PPA occupy similar positions in PPE and PPA complexes with displacement of 0.42 Å. One of the most differences is seen at the position of Cα atoms of the Glu and AAA moieties of PPE and PPA. The Cα atom of the Glu moiety moves 0.80 Å from the position of the Cα atom of the AAA moiety. Accompanied by this movement, the N atom of PPE and Nζ atom of Lys238 are displaced 0.46 and 0.83 Å, respectively. The PLP moiety of PPE was also recognized in the same way as that of PPA (Fig. 3B).

AAA-AT recognizes both AAA and Glu as amino donors with a decreased K_m value of Glu (Table 3); however, negligible activity was observed for Asp, which is one methylene unit shorter than Glu. When kinetic analysis was performed for Asp at a fixed concentration (1 mM) of 2-OG, the K_m value for Asp and the k_{cat} value for the reaction were determined to be 381 ± 61 mM and 0.046 ± 0.005 s^{-1}, respectively. Arg23 from α2 helix recognizes the side-chain carboxylates of PPE and PPA at almost the same position. The markedly larger K_m value of Asp, 820 and 470-fold larger than those of Glu and AAA, respectively, suggests that Arg23 cannot bind the β-carboxyl group of Asp tightly. Therefore, it is suggested that although α2 helix is highly flexible to accept various amino acids, no further dislocation of the helix suitable for binding the shorter side chain of Asp is allowed. Furthermore, considering that recognition by Arg23 of the γ-carboxyl group of the Glu moiety of PPE dislocates the Cα atom of the Glu moiety as described above, we presume that the Cα atom of Asp must be located apart

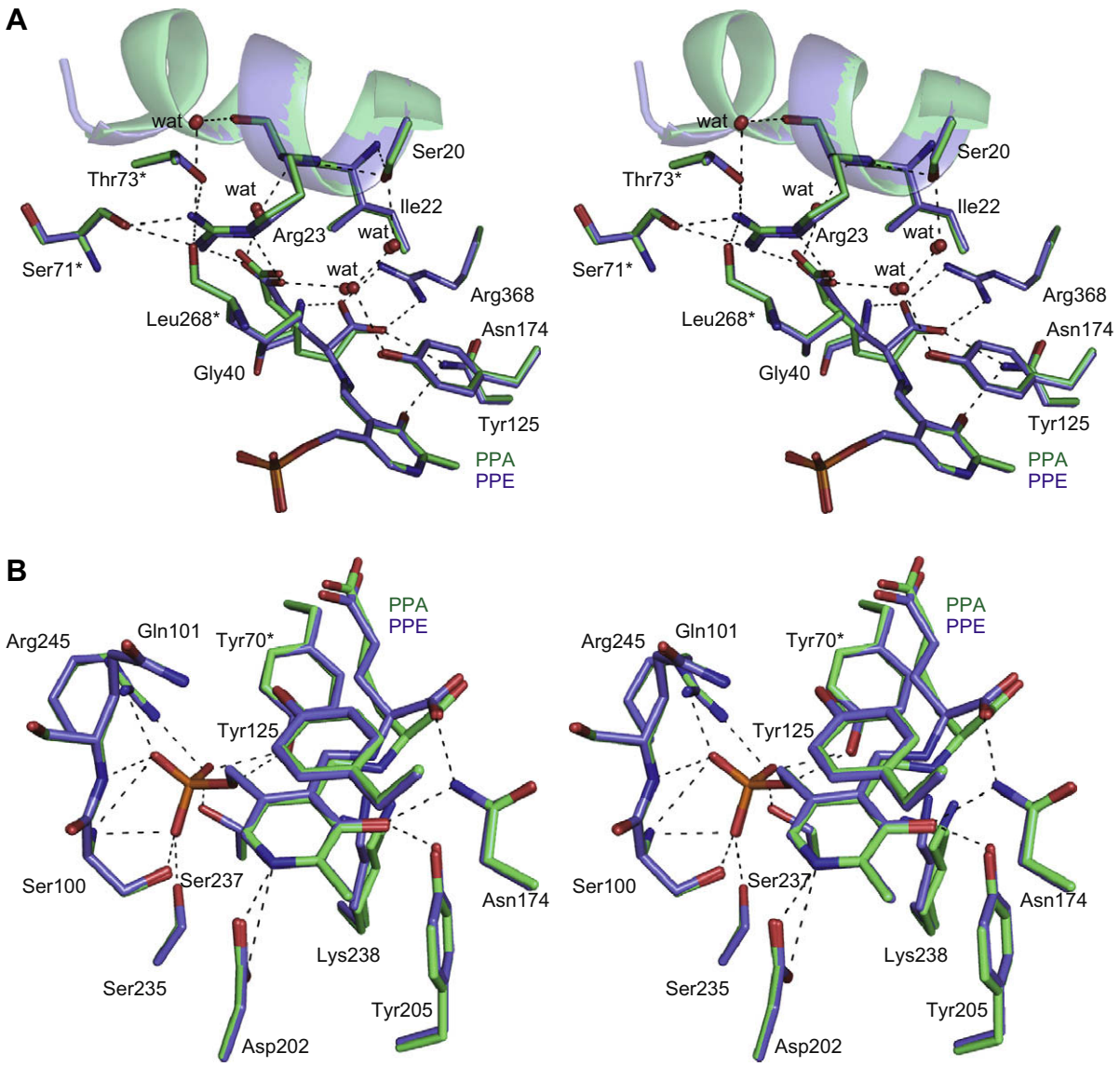

Fig. 3. Active site structure of PPE complex superposed on PPA complex. The PPE complex and PPA complex are in purple and green, respectively. (A) Stereo diagram of structure around the Glu or AAA moiety and α2 helix. α2 helix is represented in sketch format. (B) Stereo diagram of structure around PLP moiety.

Table 3
Kinetic parameters of AAA-AT variants.

Enzyme	Substrate	K_m (mM)	k_{cat} (s^{-1})	k_{cat}/K_m ($M^{-1}\ s^{-1}$)
Wild type	AAA	0.81 ± 0.06	6.7 ± 0.1	$(8.2 \pm 0.6) \times 10^3$
	2-OG	0.30 ± 0.02		$(2.2 \pm 0.1) \times 10^4$
	Leu	0.95 ± 0.08	5.1 ± 0.2	$(5.4 \pm 0.5) \times 10^3$
	2-OG	0.27 ± 0.02		$(1.9 \pm 0.1) \times 10^4$
	Glu	0.46 ± 0.05	16 ± 1	$(3.7 \pm 0.4) \times 10^4$
	2-OIC	0.43 ± 0.04		$(3.4 \pm 0.4) \times 10^4$
S20E	AAA	7.0 ± 0.6	0.040 ± 0.003	5.7 ± 0.6
	2-OG	0.41 ± 0.05		$(9.7 \pm 1.3) \times 10$
	Leu	0.20 ± 0.02	0.023 ± 0.001	$(1.2 \pm 0.1) \times 10^2$
	2-OG	0.40 ± 0.02		$(6.0 \pm 0.3) \times 10$
	Glu	82 ± 7	1.2 ± 0.1	$(1.4 \pm 0.1) \times 10$
	2-OIC	0.050 ± 0.004		$(2.4 \pm 0.2) \times 10^4$
R23A	AAA	3.3 ± 0.5	0.011 ± 0.001	3.3 ± 0.5
	2-OG	0.54 ± 0.08		$(2.1 \pm 0.3) \times 10$
	Leu	0.39 ± 0.06	0.0090 ± 0.0004	$(2.3 \pm 0.4) \times 10$
	2-OG	0.61 ± 0.06		$(1.5 \pm 0.2) \times 10$
	Glu	250 ± 24	0.23 ± 0.01	$(9.0 \pm 1.0) \times 10^{-1}$
	2-OIC	0.048 ± 0.005		$(4.8 \pm 0.6) \times 10^3$
R23Q	AAA	11 ± 1	0.083 ± 0.008	7.5 ± 1.2
	2-OG	0.42 ± 0.07		$(2.0 \pm 0.2) \times 10^2$
	Leu	0.88 ± 0.10	0.050 ± 0.002	$(5.7 \pm 0.7) \times 10$
	2-OG	0.55 ± 0.06		$(9.1 \pm 1.1) \times 10$
	Glu	62 ± 7	0.50 ± 0.03	8.1 ± 1.0
	2-OIC	0.091 ± 0.013		$(5.5 \pm 0.9) \times 10^3$

from the position suitable for the reaction even when Asp is bound to AAA-AT.

Characterization of conserved Arg23 and Ser20 in α2 helix

In the α2 helix of AAA-AT, Ser20 and Arg23 are highly conserved among AAA-AT homologues. In PPE and PPA complexes, the guanidinium group of Arg23 recognizes a substrate and forms a hydrogen-bond network with neighboring residues, as described above. The hydroxyl group of Ser20 forms a hydrogen bond with the main chain amide of Arg23 (Fig. 3A). In contrast, these interactions are lost in the PPL complex. In the PPL complex, the side chain of Arg23 extends its side-chain in the direction opposite to the active site and forms a hydrogen-bond network with Glu74* and Gln257* from another subunit (Fig. 4A). The hydroxyl group of Ser20 forms a hydrogen bond with the side-chain amide of Gln261* and the

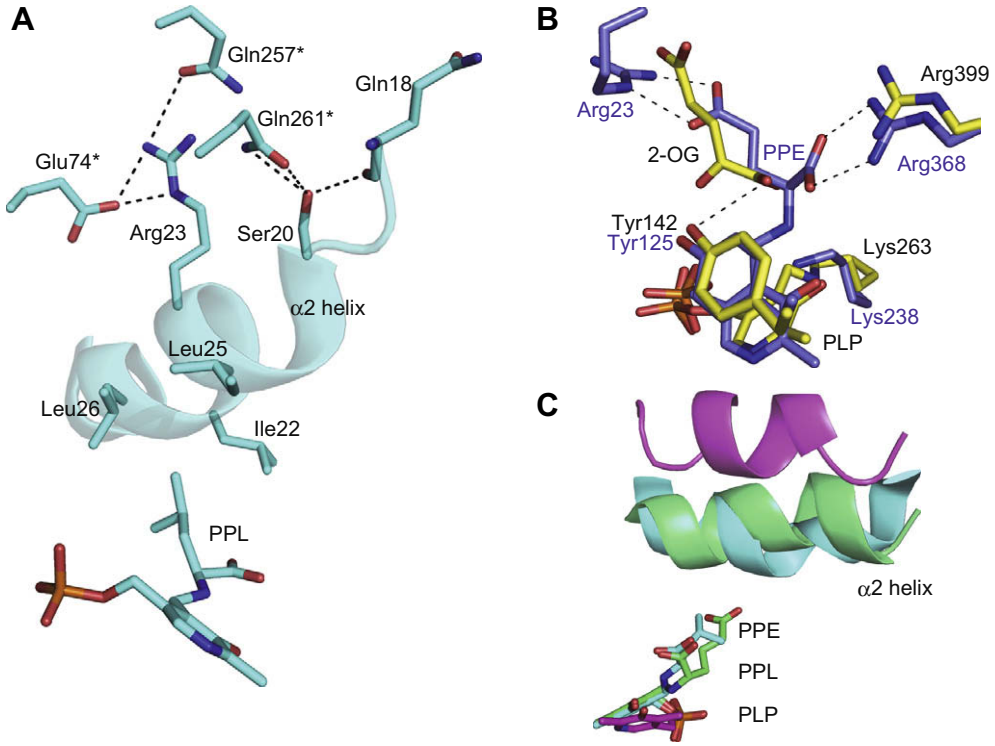

Fig. 4. Structural difference around α2 helix. (A) the PPL complex. (B) Superposition of the PPE complex of AAA-AT (purple) on hKat II/2-OG complex (yellow). Amino acid residues from AAA-AT and hKat II are indicated by purple and black letters. (C) Open and closed form of AAA-AT. The PLP complex (open form), the PPL complex, and the PPA complex (closed form) are in magenta, cyan, and green, respectively.

main-chain amide of Gln18. These structural studies revealed that Arg23 and Ser20 play dual roles in recognizing two different types of amino acids. When hydrophobic compounds are entered into the substrate-binding pocket, the Arg23/Ser20 pair functions to orient the hydrophobic surface of α2 helix toward the hydrophobic side-chain of the substrates. On the other hand, Arg23 directly recognizes the side-chain carboxyl group of acidic compounds like AAA and Glu with the aid of Ser20. To verify this hypothesis, we constructed Arg23Ala, Arg23Gln and Ser20Glu mutants and determined their kinetic parameters.

We determined the K_m and k_{cat} values of those enzymes for three combinations of substrates: AAA and 2-OG, Leu and 2-OG, Glu and 2-oxoisocaproate (2-OIC) (Table 3). Mutations Arg23Ala and Arg23Gln caused 4.1-fold and 13.7-fold increases in the K_m values for AAA, respectively. The increase in the K_m value for Glu is more prominent in Arg23Ala and Arg23Gln mutants. The K_m values for Glu increased 546-fold and 134-fold in Arg23Ala and Arg23Gln, respectively. In contrast, the K_m value for Leu was not greatly affected by the mutations; 2.5-fold and 1.1-fold decrease by Arg23Ala and Arg23Gln mutations, respectively. These results accord with the two different types of crystal structures; one is seen in the crystal structures of PPE and PPA complexes where Arg23 directly interacts with the carboxyl groups of AAA and Glu (Fig. 3A), and the other is seen in the crystal structures of PPL and Leu complexes where Arg23 is not involved in direct recognition of the Leu moiety (Fig. 4A). Interestingly, K_m values for 2-OG, which has the same chain length as Glu, of Arg23Ala and Arg23Gln mutants were similar to that of WT, contrasting with the great increase in K_m values for Glu in these mutants. This observation suggests that 2-OG is recognized in a different way although the chain length is the same between Glu and 2-OG. It should be noted that the K_m values for 2-OIC decreased by 9.0-fold and 4.7-fold in Arg23Ala and Arg23Gln mutations, respectively. This result contrasts with the observation that these mutations had a mild effect on the K_m values for Leu, which has the same side-chain as 2-OIC. This result also emphasizes that substrates with 2-amino groups and their structural homologs with 2-oxo groups are recognized by the enzyme in a different way. This hypothesis is supported by recent structural analysis of human kynurenine aminotransferase II (hKat II), an AAA-AT homolog [19,20]. When the structure of the PPE complex of AAA-AT is superimposed on that of the hKat II/2-OG complex (Fig. 4B), 2-OG is bound near PLP in hKat II; however, the α-carboxyl group is not recognized by Arg399 corresponding to Arg368 in AAA-AT, but bound to Tyr142. Furthermore, the α-carboxyl group of bound 2-OG is located apart from PLP in hKat II. Since Arg20 corresponding to Arg23 in AAA-AT is not seen in the hKat II crystal structures due to disorder of region 15–20, we cannot conclude that the residue is involved in recognition of the α-carboxyl group of 2-OG in hKat II. In any cases, all these observations and our kinetic data are consistent with the assumption that the 2-OG and Glu are recognized in a different way.

The k_{cat} value was decreased by 32- to 600-fold by the mutations of Arg23. In aspartate aminotransferase from *E. coli*, torsion between the pyridine ring and the imine bond of PLP-Lys258 aldimine is shown to be a principal factor that affects the catalytic function [21,22]. In the crystal structures of AAA-AT, Arg23 interacts with several neighboring residues (Figs. 3A and 4B); therefore, the marked decrease in the k_{cat} value can be interpreted as the result of loss of function of amino acid residues at position 23 in placing α2 helix at appropriate positions to maintain the distorted structure for efficient reaction.

Although Ser20 does not recognize AAA and Glu directly, replacement of Ser20 altered the enzyme to exhibit parameters similar to those of Arg23 mutant. In PPA and PPE complexes, Ser20 forms a hydrogen bond with the main-chain amide of Arg23 by its hydroxyl group (Fig. 3A). We speculated that Ser20 might stabilize the Arg23-N location, which allows Arg23 to have tight ionic interactions with acidic substrates. In the PPL complex, Ser20 is hydrogen-bounded with Gln261* from another subunit (Fig. 4A). In this complex, neighboring Glu257* forms a hydrogen bond with Arg23. In both cases, Ser20 also plays a crucial role in placing the substrates at appropriate position in the active site indirectly. When the substrate is bound, α2 helix occupies similar position to cover the active site, forming a closed form, whereas in the PLP complex without substrate, the helix is displaced 5–6 Å to open the active site cleft (open form) (Fig. 4C). Thus, AAA-AT adopts closed or open form in the presence or the absence of substrate. The crystal structures and site-directed mutagenesis revealed that the conserved pair of Arg23 and Ser20 plays important roles in not only direct binding of AAA and Glu but also closed form formation in AAA-AT.

Acknowledgments

This work was supported in part by a Grant-in-Aid for scientific research from the Ministry of Education, Culture, Sports, Science, and Technology of Japan, from Nagase Science and Technology Foundation, from the Asahi Glass Foundation, and from the Charitable Trust Araki Medical and Biochemistry Memorial Research Promotion Fund. This work was performed under approval of the Photon Factory Program Advisory Committee (Proposal No. 07G530). We also appreciate the staff of the Photon Factory for their assistance with data collection.

References

[1] H.E. Umbarger, Amino acid biosynthesis and its regulation, Ann. Rev. Biochem. 47 (1978) 532–606.
[2] M. Strassman, S. Weinhouse, Biosynthetic pathways. III. The biosynthesis of lysine by *Torulopsis utilis*, J. Am. Chem. Soc. 75 (1953) 1680–1684.
[3] H.J. Vogel, Distribution of lysine pathway among fungi: evolutionary implications, Am. Natl. 98 (1964) 446–455.
[4] N. Kobashi, M. Nishiyama, M. Tanokura, Aspartate kinase-independent lysine synthesis in an extremely thermophilic bacterium, *Thermus thermophilus*: lysine is synthesized via α-aminoadipic acid not via diaminopimeric acid, J. Bacteriol. 181 (1999) 1713–1718.
[5] J. Miyazaki, N. Kobashi, M. Nishiyama, H. Yamane, Functional and evolutionary relationship between arginine biosynthesis and prokaryotic lysine biosynthesis through α-aminoadipate, J. Bacteriol. 183 (2001) 5067–5073.
[6] H. Nishida, M. Nishiyama, N. Kobashi, T. Kosuge, T. Hoshino, H. Yamane, A prokaryotic gene cluster involved in synthesis of lysine through the amino adipate pathway: a key to the evolution of amino acid biosynthesis, Genome Res. 9 (1999) 1175–1183.
[7] A.B. Brinkman, S.D. Bell, R.J. Lebbink, W.M. de Vos, J. van der Oost, The *Sulfolobus solfataricus* Lrp-like protein LysM regulates lysine biosynthesis in response to lysine availability, J. Biol. Chem. 277 (2002) 29537–29549.
[8] T. Miyazaki, J. Miyazaki, H. Yamane, M. Nishiyama, α-Aminoadipate aminotransferase from an extremely thermophilic bacterium *Thermus thermophilus*, Microbiology 150 (2004) 2327–2334.
[9] T. Tomita, T. Miyagawa, T. Miyazaki, S. Fushinobu, T. Kuzuyama, M. Nishiyama, Mechanism for multiple-substrates recognition of α-aminoadipate aminotransferase from *Thermus thermophilus*, Proteins 75 (2009) 348–359.
[10] K. Haruyama, T. Nakai, I. Miyahara, K. Hirotsu, H. Mizuguchi, H. Hayashi, H. Kagamiyama, Structures of *Escherichia coli* histidinol-phosphate aminotransferase and its complexes with histidinol-phosphate and *N*-(5′-phosphopyridoxyl)-L-glutamate: double substrate recognition of the enzyme, Biochemistry 40 (2001) 4633–4644.
[11] M.M. Islam, M. Goto, I. Miyahara, K. Hirotsu, H. Hayashi, Binding of C5-dicarboxylic substrate to aspartate aminotransferase: implications for the conformational change at the transaldimination step, Biochemistry 44 (2005) 8218–8229.
[12] Z. Otwinowski, W. Minor, Processing of X-ray diffraction data collected in oscillation mode, Methods Enzymol. 276 (1997) 307–326.
[13] A. Vagin, A. Teplyakov, MOLREP: an automated program for molecular replacement, J. Appl. Crystallogr. 30 (1997) 1022–1025.
[14] Collaborative Computational Project, Number 4, The CCP4 suite: Programs for protein crystallography, Acta Crystallogr. D 50 (1994) 760–763.
[15] P. Emsley, K. Cowtan, Coot: model-building tools for molecular graphics, Acta Crystallogr. D 60 (2004) 2126–2132.
[16] G.N. Murshudov, A.A. Vagin, E.J. Dodson, Refinement of macromolecular structures by the maximum-likelihood method, Acta Crystallogr. D 53 (1997) 240–255.

[17] R.A. Laskowski, M.W. MacArthur, D.S. Moss, J.M. Thornton, PROCHECK: a program to check the stereochemical quality of protein structures, J. Appl. Crystallogr. 26 (1993) 283–291.
[18] W.W. Cleland, Statistical analysis of enzyme kinetic data, Methods Enzymol. 63 (1979) 103–138.
[19] Q. Han, T. Cai, D.A. Tagle, H. Robinson, J. Li, Substrate specificity and structure of human aminoadipate aminotransferase/kynurenine aminotransferase II, Biosci. Rep. 28 (2008) 205–215.
[20] Q. Han, H. Robinson, J. Li, Crystal structure of human kynurenine aminotransferase II, J. Biol. Chem. 283 (2008) 3567–3573.
[21] H. Hayashi, H. Mizuguchi, H. Kagamiyama, The imine-pyridine torsion of the pyridoxal 5′-phosphate Schiff base of aspartate aminotransferase lowers its pK_a in the unliganded enzyme and is crucial for the successive increase in the pK_a during catalysis, Biochemistry 37 (1998) 15076–15085.
[22] H. Hayashi, H. Mizuguchi, I. Miyahara, Y. Nakajima, K. Hirotsu, H. Kagamiyama, Conformational change in aspartate aminotransferase on substrate binding induces strain in the catalytic group and enhances catalysis, J. Biol. Chem. 278 (2003) 9481–9488.